IEICE TRANS. COMMUN., VOL.E91–B, NO.10 OCTOBER 2008

PAPER

Optical Cross-Connect Switch Architectures for Hierarchical Optical Path Networks

Shoji KAKEHASHI[†], **Hiroshi HASEGAWA**[†a)], ***Members***, ***and*** **Ken-ichi SATO**[†b)], ***Fellow***

SUMMARY This paper proposes new switch architectures for hierarchical optical path cross-connect (HOXC) systems. The architectures allow incremental expansion of system scale in terms of the number of input/output fiber ports, wavebands, and optical paths per waveband. These features assure the cost-effective introduction of HOXCs even at the outset when traffic volume is not so large. Furthermore the effectiveness of the proposed switch architectures is demonstrated in a comparison with single-layer OXCs (conventional OXCs). The results provide useful criteria for the introduction of HOXCs in terms of hardware scale.

key words: *waveband, waveband cross-connect, optical cross-connect*

1. Introduction

Broadband access including ADSL and FTTH is being rapidly adopted throughout the world and, as a result, traffic is continually increasing. The maximum number of WDM wavelengths per fiber now exceeds one hundred, and wavelength routing using ROADMs (Reconfigurable OADMs) is being widely adopted to develop cost-effective networks [1]. GMPLS controlled OXCs have also been used to create nation-wide testbeds [2]. Further traffic expansion is expected in the near future with the introduction of new broadband services including IP TV and high definition TV. This will result in a significant increase in the number of wavelength paths that are to be cross-connected at nodes, and hence optical node throughput needs to be greatly enhanced. To resolve this problem, the hierarchical optical path cross-connect (HOXC) [3]–[5] is being investigated; it can handle hierarchical bandwidth optical paths, wavelength paths and wavebands (WBs) which consist of multiple wavelength paths. Indeed, several studies have targeted the development of hierarchical optical path network design algorithms [6]–[9], these algorithms were shown to greatly lower network cost compared to conventional single-layer optical path networks for a wide range of traffic demand. Most of the works evaluated the effectiveness in terms of the total number of OXC and HOXC ports compared to those of single-layer OXCs. Another study [10] showed that an HOXC with non-uniform WB size can not only improve node throughput but also reduce cross-connect node cost.

The key components needed to develop HOXCs are waveband multi/demultiplexers (WB MUX/DEMUX), waveband cross-connects (BXCs) and wavelength path cross-connects (WXCs). Some architectures for WB MUX/DEMUX have been proposed; they use an Arrayed-Waveguide Grating [11]–[13], a thin-film filter [14], and concatenated AWGs [15], [16]. A major omission is the failure to resolve which switch architecture, including BXC and WXC, is most effective in minimizing switch scale and maximizing flexibility and cost reduction. To create an optical switch, different switch architectures and technologies have been utilized. They include 2-dimensional [17] and 3-dimensional (3D) MEMS [18], a PLC (Planar Light-wave Circuit) [19] switch, and a mechanical fiber switch. The 3D MEMS switch is attractive due to its high functionality and low optical insertion loss and crosstalk [20]. However, the micro mirrors must be controlled in three dimensions and require extreme assembly and operation precision; reliability in various conditions needs to be verified. On the other hand 2D MEMS and PLC switches (two dimensional matrix type switches) are attractive because of their proven reliability [21] and high productivity. The PLC switches are in wide-spread commercial use [22], [23]. This paper, therefore, focuses on BXC and WXC architectures assuming the use of the latter switch technologies.

Specific HOXC architectures have not been discussed in detail so far, nor has the best combination of BXC and WXC switches been identified. Accordingly, the comparison of the switch scales of HOXCs and single-layer OXCs has been insufficient. One of the key requirements of both types of switches, excellent scalability, has not been discussed with regard to HOXC switches. This feature assures the cost-effective introduction of HOXCs, even at the outset when traffic volume is not so large, while allowing for graceful expansion in accordance with later traffic growth. This paper tackles the above unresolved problems and proposes novel switch architectures for HOXC that not only require fewer switching elements than single-layer OXCs, but also allow an incremental increase in the number of input/output fiber ports, wavebands, and wavelength paths per waveband.

First, we investigate the various switch architectures and discuss scalability for the single-layer OXC and HOXC. This paper then elucidates the most attractive switch architectures for single-layer OXCs and HOXCs, considering the number and type of switch elements and flexibility. A detailed comparison allows us to clarify the conditions under which HOXC are more cost-effective than single-layer OXCs.

Manuscript received July 18, 2007.
Manuscript revised March 27, 2008.

[†]The authors are with Nagoya University, Nagoya-shi, 464-8603 Japan.
a) E-mail: hasegawa@nuee.nagoya-u.ac.jp
b) E-mail: sato@nuee.nagoya-u.ac.jp

DOI: 10.1093/ietcom/e91–b.10.3174

2. Switch Architectures

2.1 Basic Node Architecture

In a single-layer OXC, wavelength paths are de-multiplexed by DEMUX, routed by a WXC, and then combined by MUX (See Fig. 1). Wavelength converters can be inserted before or after the WXC so as to avoid wavelength collision. We will not take this scheme into consideration because wavelength converters are expensive and wavelength collisions can be greatly decreased by applying effective routing algorithms. Here, blocking does not include the blocking caused by wavelength collision between input and output ports, which can occur in optical path routing. The non-blocking characteristics are classified [24], [25] into strictly non-blocking, non-blocking in a wide sense, and rearrangeable non-blocking. A switch is strictly non-blocking if any input can always be connected in any viable way to any unused output without disturbing existing connections. In this paper, our proposed switch architectures utilize non-blocking switches.

An HOXC is divided into two parts as shown in Fig. 2. One part consists of WB MUX/DEMUX and BXC for routing higher-order waveband paths, and the other part consists of MUX/DEMUX and WXC for routing lower-order wavelength paths. The routing of optical paths should be processed by BXC as much as possible so as to decrease HOXC switch scale. In other words, the WXC part should only be used when the routing of optical path cannot be processed by just BXC. To attain this, we need to create

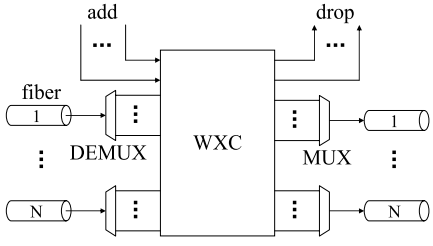

Fig. 1 Generic configuration of single-layer OXC.

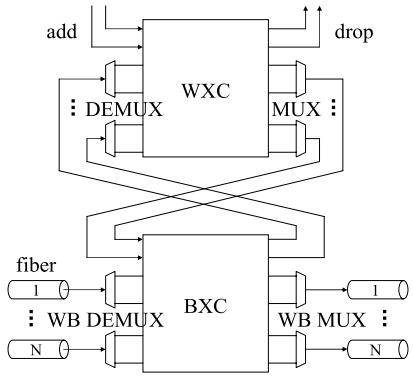

Fig. 2 Generic configuration of HOXC.

effective network design algorithms, accommodate wavelength paths into wavebands and accommodate wavebands into fibers [6], [7]. Several studies [5], [26] proposed non-hierarchical OXCs where wavelength paths and WBs are accommodated simultaneously in a fiber. This system is optimal for a fixed condition, but cannot adapt to traffic demand changes at all, so we don't consider this arrangement here.

2.2 Measure of Switch Scale

Because the internal architectures of BXC and WXC have not been clarified yet, most previous studies employed the total number of input and output fiber ports as the measure with which to compare switch sizes. This measure, however, is not adequate because switch complexity is not necessarily proportional to the number of ports. In this paper, we take the number of equivalent 1×2 element optical switches as the measure used to evaluate total switch complexity. For example, a 2×2 Mach-Zehnder interferometer [27] is regarded as two 1×2 switches so its size is counted as two. In the case of the $N \times N$ matrix switch, it requires N^2 of 2×2 switch elements, that is, $2N^2$ 1×2 switch elements.

2.3 Kinds of Flexibility in Single-Layer OXC

To realize the economical introduction of optical cross-connects and their subsequent expansion to cope with traffic growth, the system must offer modular growth capability. We considered the following attributes of expansion in single-layer OXC.

1) Modular growth regarding the number of fibers: The number of input/output fiber ports is incrementally increased as traffic demand increases. This permits minimum initial investment with regard to fiber ports and WXC switch scale.

2) Modular growth regarding the number of wavelength paths per fiber: The number of wavelength paths per fiber is incrementally increased as traffic demand increases. This minimizes initial investment with regard to the ports connecting MUX/DEMUX and WXC and WXC switch scale.

3) "Colorless" add/drop capability of wavelength paths from/to electrical systems: Any wavelength path(s) can be added from or dropped to electrical systems (Digital Cross-Connect Systems or routers, etc.). This is called the colorless add/drop capability of wavelength paths from/to electrical systems [28]. This optimizes the number of required add/drop ports from/to electrical systems.

2.4 Four Single-Layer OXC Switch Architectures

This section presents four single-layer OXC switch (SW) architectures and clarifies which is optimal in terms of cost, loss, and flexibility. Let N be the number of input/output fibers and M be the number of wavelength paths per fiber. A variable x is introduced to stand for the ratio of wavelength paths: the proportion of the number of wavelength paths to

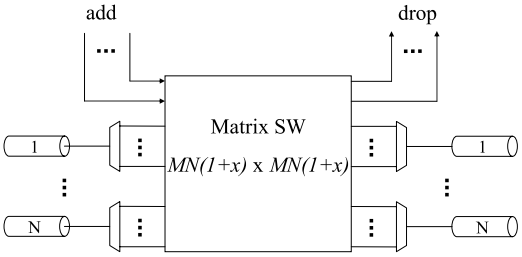

Fig. 3 Single-layer OXC with a large matrix switch.

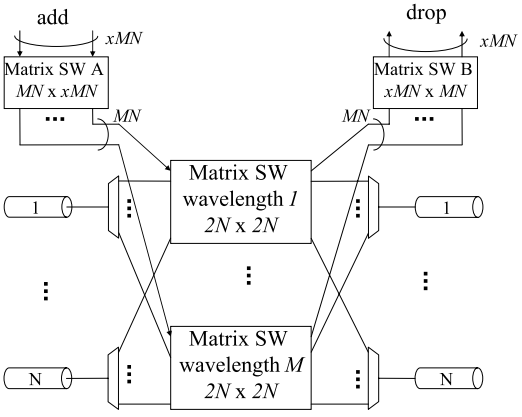

Fig. 4 Single-layer OXC that consists of matrix switches dedicated to the same-wavelength paths and $MN \times xMN$ matrix switches restricting the number of add/drop wavelength paths.

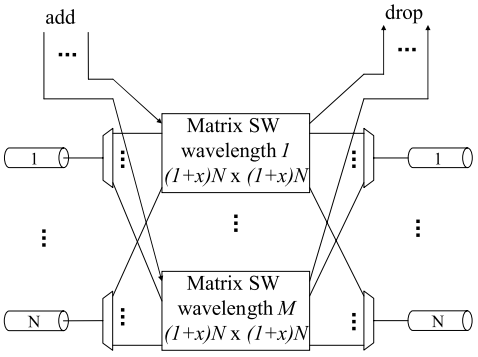

Fig. 5 Single-layer OXC that consists of matrix switches dedicated to the same-wavelength paths (the number of add/drop wavelength paths is fixed within each path group).

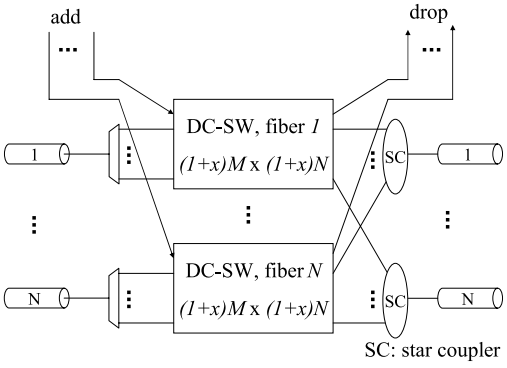

Fig. 6 Single-layer OXC that uses DC-SWs.

be added/dropped for connections to electrical systems to that coming/outgoing to/from the node.

Figure 3 shows a single-layer OXC with a large $MN(1 + x) \times MN(1 + x)$ matrix switch. It is possible to route optical paths from any input port to any output port. The configuration has colorless add/drop capability of wavelength paths as described in Sect. 2.3, however, requires a large switch scale in terms of the number of necessary element switches.

Figure 4 shows a single-layer OXC that has a $2N \times 2N$ matrix switch for each optical path group with the same wavelength and two $xMN \times MN$ matrix switches that can restrict the number of add/drop wavelength paths in a colorless fashion. The number of $2N \times 2N$ matrix switches, M, equals to the maximum number of wavelength paths that can be accommodated per fiber. Each $2N \times 2N$ switch assigns an output fiber port to each wavelength path. The matrix switch A (Fig. 4) can limit the number of routed wavelength paths from electrical systems to WXC, and B (Fig. 4) can limit the number of routed wavelength paths from WXC to electrical systems. This architecture provides the same switch function as a single large matrix switch (shown in Fig. 3) and allows a significant switch scale reduction compared to that possible with a single large matrix switch (numerical evaluations will be given later).

Figure 5 shows a single-layer OXC that has a $N(1 + x) \times N(1 + x)$ matrix switch for each optical path group with the same wavelength. The number of matrix SWs, M, equals to number of wavelength paths per fiber. Each $N(1 + x) \times N(1 + x)$ SW assigns an output fiber port to each wavelength path. This architecture imposes a limit in terms of add/drop capability; ratio x is fixed within each wavelength path group. It is found that this limitation can, however, greatly reduce the total switch scale compared to that in Fig. 4. In addition, the configuration provides good modular growth capability in terms of wavelength path number.

Figure 6 shows a single-layer OXC that uses Delivery and Coupling Switches (DC-SWs) [25], [29]. This OXC utilizes N, $M(1 + x) \times N(1 + x)$ DC-SWs and one switch is dedicated to each input fiber. A matrix type arrangement of the $M \times N$ DC-SW is shown in Fig. 7(a) and a tree type arrangement is shown in Fig. 7(b). These switch configurations were originally proposed in 1994 [29] and used in optical cross-connect systems that have been utilized to create nation wide testbed networks [30]. The DC-SW architecture is the same as that of WSS (Wavelength Selective Switch). The large scale deployment WSS for ROADM systems is underway [31]. In Figs. 7(a) and (b), N MUXs are used when the wavelength of each input signal is fixed; note that an optical star coupler can be used instead of the MUX when the wavelength of each input signal is not fixed or can change (wavelength conversion is employed). The DC-SW allows any of the M incoming optical signals to be connected to any of the N outgoing ports. These outgoing

port signals are coupled to output fiber ports by using a star coupler (SC) as shown in Fig. 6. This architecture limits the add/drop ratio of the optical paths to x regarding each fiber. It is found that with this limitation the necessary switch scale can be much smaller than that in Fig. 4 (numerical evaluations are given later). This configuration provides excellent modular growth capability in terms of input and output fiber pairs [25], [29].

The switch scale for each architecture (Fig. 3–Fig. 6) is formulated in Appendix. The formulations are derived from the total number of 1×2 switch elements of all matrix switches (the measure of switch scale is given in Sect. 2.2).

2.5 Comparison of four Single-Layer OXC Switch Architectures

Table 1 summarizes the required number of MUXs/ DEMUXs and star couplers, and explains what kinds of flexibility are available from different architecture single-layer OXCs. Figures 8(a), (b) and (c) show comparisons of switch scale in terms of the number of necessary element switches for each single-layer OXC, where M, N and x are changed respectively. The switch scale is exact when a parameter, for example $(1 + x)N$, is an integer. But when $(1 + x)N$ is not an integer, the switch scale can be approximated by the extrapolated values of those for exact integer values. The results in Fig. 8 are the approximated values when parameters are not integers. It is found that for the single-layer OXC

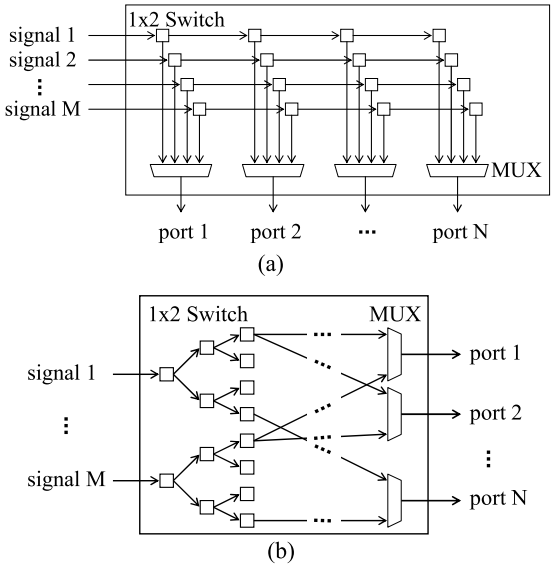

Fig. 7 Different DC-SW arrangements. (a) Matrix type $M \times N$ DC-SW. (b) Tree type $M \times N$ DC-SW.

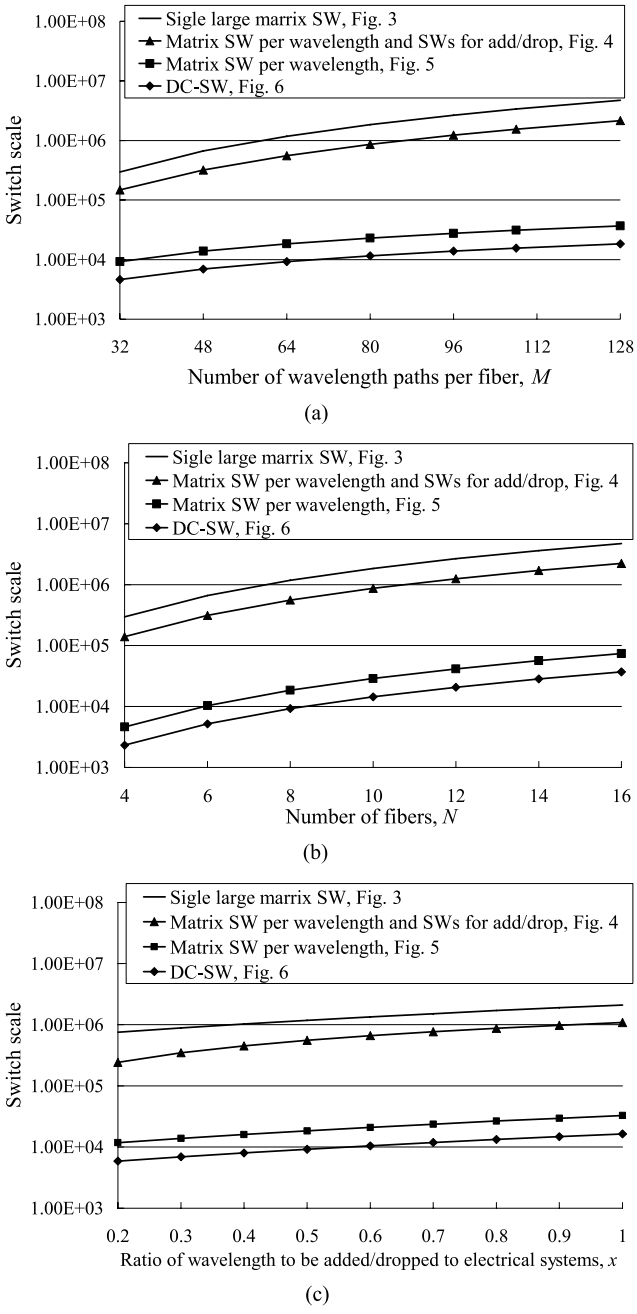

Fig. 8 Comparisons of SW scale for different single-layer OXC SW architectures. (a) $N = 8$, $x = 0.5$. (b) $M = 64$, $x = 0.5$. (c) $N = 8$, $M = 64$.

Table 1 Comparison of single-layer OXC switch architectures.

Single-layer OXC SW architecture	Figure	# of MUX/DEMUX	# of SC	Kinds of flexibility
Single large matrix SW	Fig. 3	$2N$	-	- Colorless add/drop capability of wavelength paths
Matrix SW per wavelength and SWs for add/drop	Fig. 4	$2N$	-	- Colorless add/drop capability of wavelength paths
Matrix SW per wavelength	Fig. 5	$2N$	-	- Modular growth regarding the number of wavelength paths
DC-SW	Fig. 6	$N(N+1)$	N	- Modular growth regarding the number of fibers - Colorless add/drop capability of wavelength paths in each fiber

with a large matrix switch (Fig. 3) and with a matrix SW per wavelength and SWs for add/drop (Fig. 4), the switch scale is about ten times bigger than that of any of the other single-layer OXC architectures considered here. DC-SW is the best in terms of SW scale, but requires many more MUXs/DEMUXs than the other architectures; the number is proportional to order N^2 because the architecture requires N DC-SWs each of which utilizes $N+1$ MUXs. This means that with present technologies (the large scale integration of optical component is not mature) the DC-SWs may not be cost-effective. The SW architecture requires N SCs which leads to $10 \log N$ dB intrinsic loss, which may be an issue when N becomes large. Moreover, since multiple wavelength paths can be delivered and dropped at a particular drop port, an additional demultiplexer is required for separating these wavelength paths. The single-layer OXC that consists of matrix SWs dedicated to the same-wavelength paths, shown in Fig. 5, can be constructed with smaller scale switches than the switch used in Fig. 3 and Fig. 4, and it uses the fewest MUXs/DEMUXs. It is found that introducing restrictions in terms of the add/drop ratio, x, so that ratio x is fixed within each wavelength path group, substantially reduces switch scale, although this restriction may slightly increase the complexity associated with network design. As a result, when demand for modularity in terms of input/output fibers is not critical, the SW architecture based on a matrix SW for each same-wavelength path group is very attractive for constructing single-layer OXCs with regard to cost (small switch scale) and loss (the small number of necessary optical devices).

2.6 Kinds of Flexibility in HOXC

To realize the economical introduction of optical cross- connects and their subsequent expansion to cope with traffic growth, the architecture must offer modular growth capability. We considered the following attributes of HOXC expansion.

1) Modular growth regarding the number of fibers: The number of input/output fiber ports is incrementally increased as traffic demand increases. This permits minimum initial investment with regard to fiber ports.

2) Modular growth regarding the number of WBs per fiber: The number of WBs per fiber is incrementally increased as traffic demand increases. This minimizes initial investment with regard to the ports that connect WB MUX/DEMUX and BXC and as a result the BXC switch scale.

3) Modular growth regarding the number of wavelength paths per WB: The number of wavelength paths per WB is incrementally increased as traffic demand increases. This minimizes initial investment with regard to the ports connecting MUX/DEMUX and WXC and as a result the WXC switch scale.

4) "Colorless" add/drop capability of WBs from/to WXC: Any waveband(s) can be added or dropped from or to WXC, which is called colorless add/drop capability regarding wavebands from/to WXC. This minimizes the number of required add/drop ports from/to WXC.

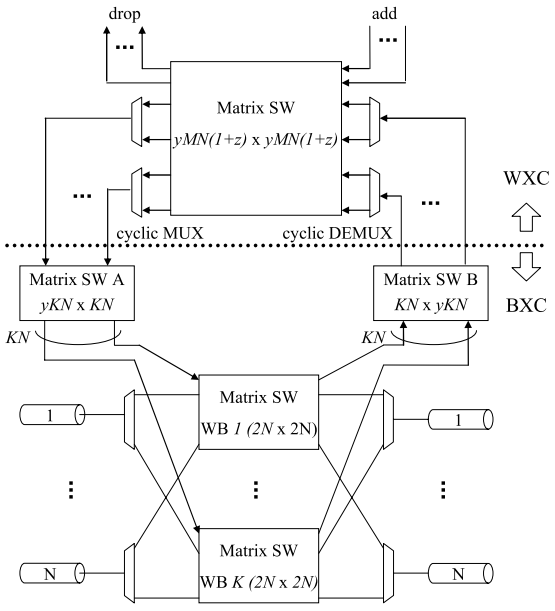

Fig. 9 BXC that has one $2N \times 2N$ matrix SW for each WB and $KN \times yKN$ matrix SWs restricting the number of add/drop WBs, and WXC with a large matrix SW.

2.7 Three HOXC Switch Architectures

In this section we present three HOXC switch architectures that are desirable in terms of cost, loss and flexibility. HOXC is divided into two parts; WXC and BXC. WXC switch architecture is influenced by BXC architecture as discussed below. Let N be the number of fibers, M that of wavelength paths per fiber, K that of WBs per fiber, and L that of wavelength paths per WB. A variable y is introduced to stand for the ratio of WBs that are dropped from BXC to WXC, to WBs that are delivered to the node (or the ratio of WBs that are added from WXC to BXC, to WBs that are launched from the node). A variable z is introduced to stand for the ratio of wavelength paths that are dropped from WXC to electrical systems, to the wavelength paths that are dropped to the WXC from BXC (or the ratio of wavelength paths that are added from electrical systems to WXC, to the wavelength paths that are added from WXC to BXC). Thus, the product of K and L equals M; y and z range from 0 to 1. The switch scale changes according to the values of y and z used. A detailed switch scale evaluation for different combinations of y and z is given in Sect. 3.

Figure 9 shows the BXC architecture consisting of $2N \times 2N$ matrix SWs, each of which is dedicated to a WB, and $KN \times yKN$ matrix SWs, which restricts the number of add/drop WBs, and a WXC with a large $yMN(1+z) \times yMN(1+z)$ matrix switch. The $yKN \times KN$ matrix switch A (Fig. 9) limits the number of WBs routed from WXC to BXC, and the $kN \times ykN$ matrix switch B limits the number of WBs routed from BXC to WXC. Owing to the $KN \times yKN$

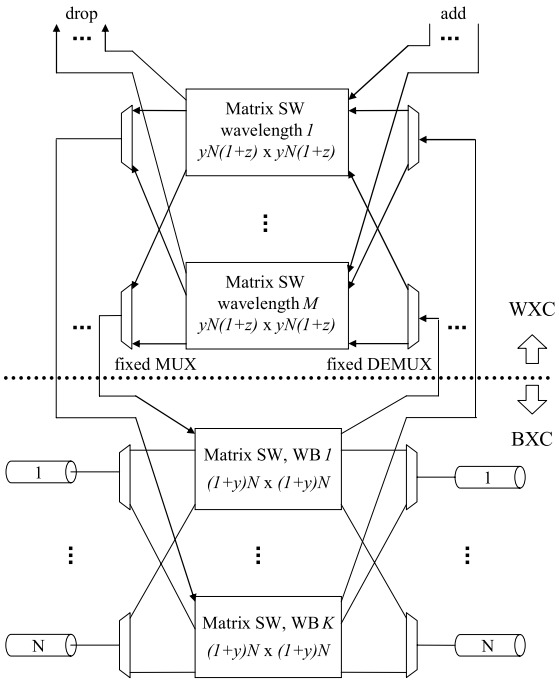

Fig. 10 BXC that consists of matrix SWs, each of which is dedicated to one WB, and WXC that consists of matrix SWs, each of which is dedicated to one wavelength.

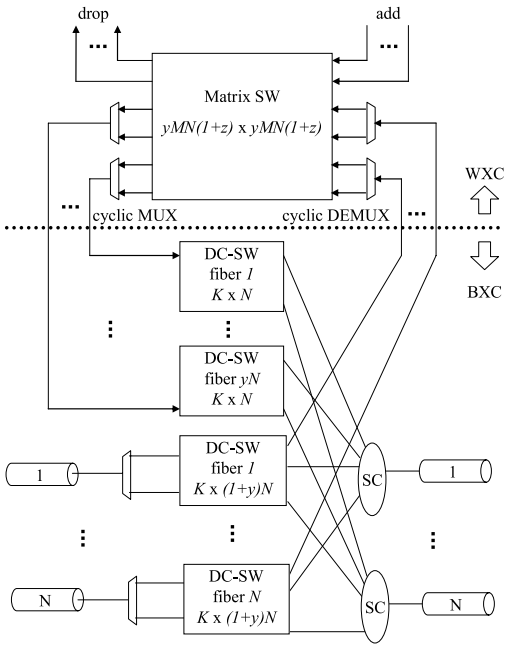

Fig. 11 BXC using DC-SWs and WXC with a large matrix SW.

matrix switches, the configuration offers colorless add/drop capability with regard to wavebands. Since colorless wavebands are input to the WXC's DEMUX, the DEMUX must have a cyclic demultiplexing capability that can accommodate any waveband(s) within a broad optical bandwidth. Such characteristics can be realized with an arrayed waveguide grating (AWG)-based DEMUX [32]. In a cyclic DEMUX, some difficulty exists in precisely aligning the channel frequencies on the ITU-T grid for any waveband in a broad optical bandwidth. Due to the above colorless nature of add/drop wavebands, there is a requirement on the WXC switch to be used with the BXC. The WXC switch must be able to route any wavelength optical paths from any input port to any output port. The WXC switch architecture that has this characteristic is shown in Fig. 3. The switch shown in Fig. 3 can route any wavelength optical paths from any input port to any output port, as discussed in Sect. 2.5, and thus the switch architecture is adopted for the WXC in combination with the BXC to create an HOXC.

Figure 10 shows the combination of BXC that has $(1 + y)N \times (1 + y)N$ matrix SWs for each WB and the WXC that has $yN(1 + z) \times yN(1 + z)$ matrix SWs for each wavelength to create an HOXC. The architecture makes the value of y equal among the different WB groups. Each $(1+y)N \times (1+y)N$ SW assigns one output port to each WB. This configuration has modular growth capability in terms of WBs. Since this architecture consists of waveband specific switches, the input waveband (the dropped waveband) to the WXC's DEMUX is fixed and hence the DEMUX can be specific to the waveband. The WXC switch architecture that should be adopted here is that shown in Fig. 5; it is one of the most attractive architectures for a single-layer OXC in terms of switch scale and has modular growth capability in terms of wavelength path level, as discussed in Sect. 2.5.

Figure 11 shows the BXC that uses $K \times (1 + y)N$ and $K \times N$ DC-SWs and the WXC with a large $yMN(1 + z) \times yMN(1+z)$ matrix switch. This architecture makes the value of y equal among different groups of fibers. One $K \times (1+y)N$ DC-SW is dedicated to each input fiber. This configuration has module growth capability in terms of fiber. Since this architecture has colorless add/drop (waveband) capability with regard to fiber, a colorless waveband is input to the WXC's DEMUX and hence the DEMUX must be a cyclic DEMUX. The WXC switch architecture that must be adopted here is that shown in Fig. 3; the same discussion holds true for the selection as was done regarding Fig. 9.

The switch scale for each architecture (Fig. 9–Fig. 11) is formulated in Appendix. The formulations are derived from the total number of 1×2 switch elements of all matrix switches (the measure of switch scale is given in Sect. 2.2).

2.8 Comparison of Three HOXC Switch Architectures

Regarding the three HOXC architectures discussed above, the necessary number of WB MUXs/DEMUXs and SCs, the necessary number and type of wavelength MUXs/DEMUXs, and the kinds of flexibility realized are summarized in Table 2. Figures 12(a) and (b) show comparisons of SW scale in each HOXC, where M is the variable in Fig. 12(a), and N is the variable in Fig. 12(b). The architectures shown in Figs. 9 and 11 require about ten times larger switch scale than the switch architecture shown in Fig. 10. Moreover, the required wavelength MUXs/DEMUXs in

Table 2 Comparison of HOXC switch architectures.

BXC SW architecture	Figure	# of WB MUX/DEMUX	Type of wavelength MUX/DEMUX (the #)	# of SC	Kinds of flexibility in HOXC
Matrix SW per WB consisting of the same wavelength paths, connected to different matrix SWs that restrict number of add/drop WBs	Fig. 9	$2N$	Cyclic ($2yKN$)	-	- Colorless add/drop capability of WBs from/to WXC - Colorless add/drop capability of wavelength paths
Matrix SW per WB consisting of the same wavelength paths	Fig. 10	$2N$	Fixed ($2yKN$)	-	- Modular growth regarding the number of wavelength paths - Modular growth regarding the number of WBs
DC-SW	Fig. 11	$N + N^2 + 2yN^2$	Cyclic ($2yN$)	N	- Modular growth regarding the number of fibers - Colorless add/drop capability of WBs from/to WXC in each fiber - Colorless add/drop capability of wavelength paths in each fiber

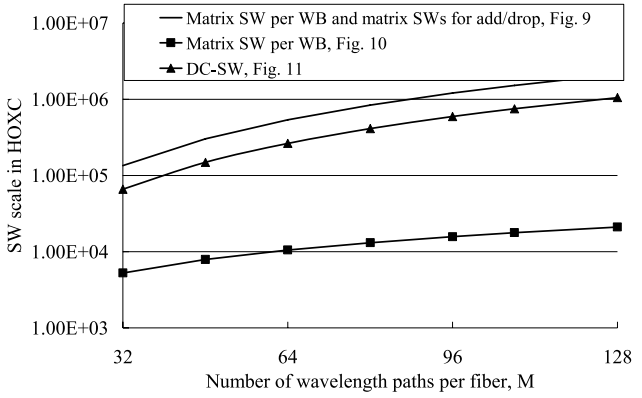

(a)

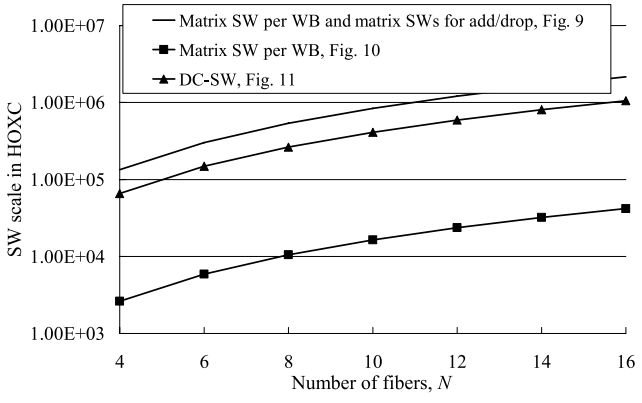

(b)

Fig. 12 Comparisons of SW scale for different HOXCs. (a) $N = 8$, $K = 8$, $y = 0.5$, and $z = 1$. (b) $M = 64$, $K = 8$, $y = 0.5$, and $z = 1$.

Figs. 9 and 11 are cyclic MUXs/DEMUXs. The necessary number of WB MUXs/ DEMUXs in the architecture shown in Fig. 11 is proportional to the second order of power$N$ because N WB MUXs are required per one DC-SW and N DC-SWs are needed to realize the cross-connect system shown in Fig. 11, which is the most rapid increase among all architectures. The SW architecture needs N SCs which produces $10 \log N$ dB intrinsic loss, which can be an issue when N is large. The architecture shown in Fig. 10 is the best in terms of SW scale and it requires the smallest number of WB

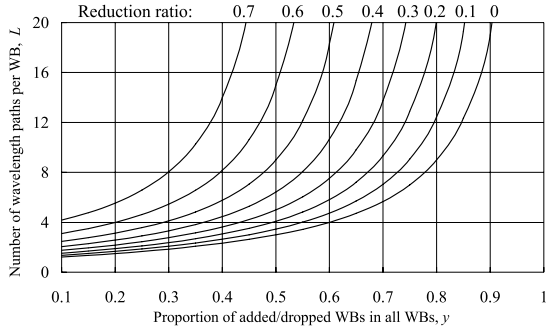

Fig. 13 The ratio of number of switch elements needed in single-layer OXC over that required by HOXC.

MUXs/DEMUXs. This architecture, therefore, offers very attractive characteristics for developing HOXCs in terms of cost, loss, and flexibility. Ratio x is fixed within each wavelength path group. The restriction regarding add/drop WBs from/to WXC within each waveband group (shown in Fig. 10) is more effective than the colorless add/drop capability of WBs from/to WXC (shown in Figs. 9 and 11) in reducing switch scale.

3. Comparisons of Switch Scale

3.1 Single-Layer OXC vs. HOXC for Transit Switch

Figure 13 shows the evaluation results for the ratio of the switch elements needed for the single-layer OXC shown in Fig. 5 and for the HOXC shown in Fig. 10. In the evaluation, the add/drop ports to/from electrical systems (digital cross-connect systems, routers, etc.) are not counted; in other words the architecture considers only the transit switch function. As depicted in Fig. 13, the reduction in HOXC switch scale over that required by the single-layer OXC is characterized by two parameters; the number of wavelength paths per WB, L, and the proportion of possible added/dropped WBs to/from WXC to all WBs delivered to the node, y. It is noted that the ratio of number of switch elements does not depend on the other parameters; the number of fibers, N, and that of wavelength paths per fiber, M, and so on. By enlarging L and/or reducing y, the

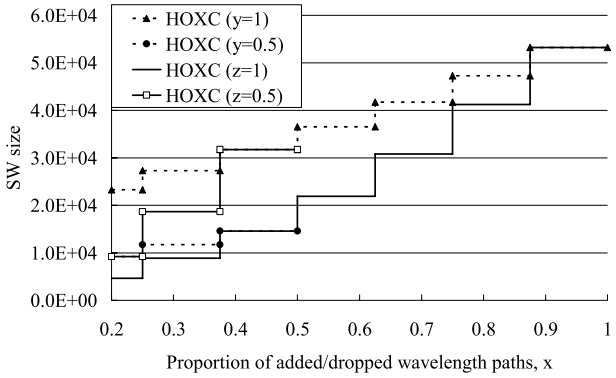

Fig. 14 Comparison of HOXC SW scale in terms of $x = yz$ ($N = 8$, $M = 96$, $K = 8$).

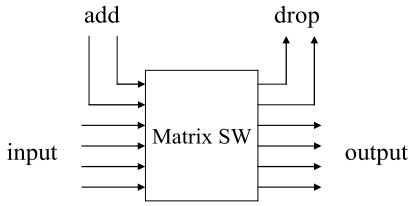

Fig. 15 Add/drop ports pertaining to matrix switch.

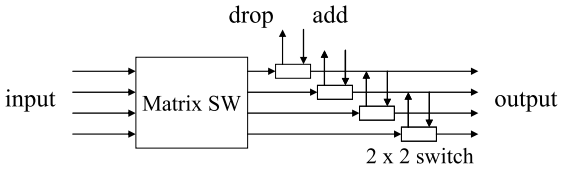

Fig. 16 Add/drop ports with 2×2 SWs.

degree of switch scale reduction is enhanced. For example, on the condition that y is lower than about 0.5 and L is larger than 6, HOXC switch scale is less than half of that of the single-layer OXC. Several previous studies [3], [33] on HOXC have proved that the value of y normally ranges from 0.2 to 0.4 in various network conditions. Within this range of y values, a useful switch scale reduction can be attained by utilizing HOXC with L values larger than 3 or 4.

3.2 The Best Way in Restricting Add/Drop Wavebands and Wavelength Paths in HOXC

For OXCs in non transit-only nodes, some of the input and output ports of a switch are used for intra-office interconnections between optical switches and electrical systems such as electrical digital cross-connect systems and routers. There are fewer add/drop ports to/from electrical systems than total wavelength paths delivered to the node. In other words, the ratio of wavelength paths to be added/dropped to/from electrical systems at a node, a variable x, is smaller than 1. As mentioned before, the value of x normally ranges from 0.2 to 0.4 for various network conditions. For HOXC, the add/drop wavelength paths between optical switches and electrical systems are restricted through two stages of switches, BXC and WXC. This is because in HOXC x equals the product of variable y and variable z, as discussed in Sect. 2.7. To minimize total optical switch scale, it is critical to identify the best combination of y and z.

Figure 14 shows a comparison of HOXC switch scale in terms of x, which equals the product y and z. In Fig. 14, x is variable (horizontal axis) and N, M and K is set at 8, 96, and 8, respectively. Either y or z is set at a constant value, 1 or 0.5 while the other is varied.

It is shown in Fig. 14 that setting z to 1 yield the smallest HOXC switch scale. This means that the restriction imposed in the BXC stage is more effective than that in the WXC stage in reducing switch scale.

In the following evaluations of HOXC switch scale, z is set at 1, in other words, the restriction is done only at the BXC stage. Comparisons are accordingly done with the condition that x for single-layer OXCs and y for HOXCs are set equal.

3.3 Single-Layer OXC vs. HOXC: Add/Drop Ports are Considered

As discussed in the previous sections, for OXCs in non transit-only nodes, intra-office interconnections between optical switches and electrical systems can significantly increase total switch scale. In order to minimize total optical switch scale, it is, therefore, essential to find a way to realize add/drop ports in an optimal manner.

Figure 15 shows a conventional way of realizing add/drop ports; those pertaining to a matrix switch. Some of the matrix SW ports are utilized as add/drop ports. Because this system can restrict the number of add/drop ports as designed, this system can minimize the number of add/drop ports. However, this system increases the matrix SW scale.

Figure 16 shows a newly proposed add/drop port arrangement based on the use of 2×2 SWs. A 2×2 SW is added to each output port of the matrix SW; this approach has been used to create ADMs, but there was no discussion of its application to OXC. With this arrangement, the matrix SW scale does not increase irrespective of the existence of add/drop ports, that is, this system can minimize the matrix SW scale. However, this arrangement cannot restrict the number of add/drop ports and allows all signals input to the matrix switch to be dropped.

In the following evaluations for HOXC, z is set to 1 as discussed before, in other words, the restriction is done only in the BXC stage (see Sect. 3.2). Comparisons are done with the condition that x for single-layer OXC and y for HOXC are set equal. Figures 17(a) and (b) show evaluated switch scale for single-layer OXC (Fig. 5) and HOXC (Fig. 10), with the two variants defined as using and not using 2×2 SWs. In Fig. 17(a), x is a variable (horizontal axis), N is set at 8, M is set at 96, and K is set at 8. In Fig. 17(b), M is set at 64, and the other parameters are same. In the single-layer OXC that uses 2×2 SWs for add/drop, the number of

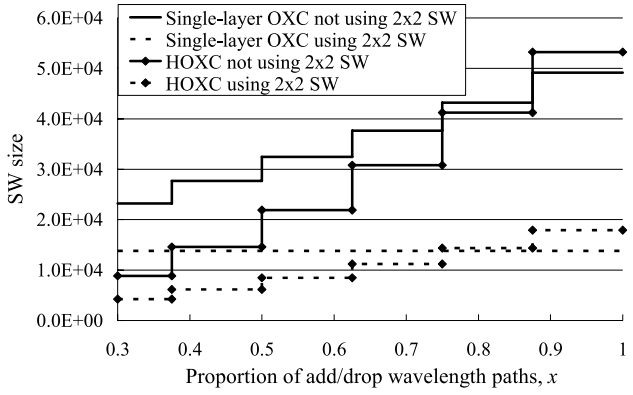

(a)

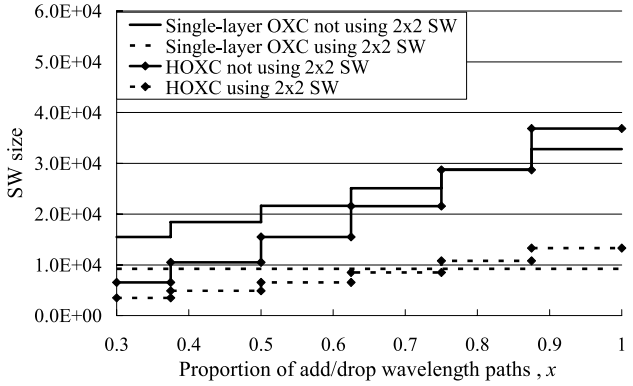

(b)

Fig. 17 Comparisons of SW scale for single-layer OXC and HOXC. (a) $N = 8$, $M = 96$, $K = 8$. (b) $N = 8$, $M = 64$, $K = 8$.

add/drop ports is constant, MN, regardless of x. It is demonstrated that by using 2×2 SWs, switch scale can be greatly reduced in both the single-layer OXC and the HOXC. This advantage becomes more prominent as x becomes bigger. Figures 17(a) and (b) elucidate the region and the conditions in which HOXCs are more effective than the single-layer OXC. When x is less than 0.5, HOXC switch scale can be 70% to 30% smaller than that of the single-layer OXC. This advantage strengthens as M becomes bigger.

4. Conclusion

Very few prior discussions have examined HOXC architecture in detail; most papers considered only the number of input/output ports. This paper has rectified this omission by investing practical HOXC architectures in detail. The different kinds of switch flexibility needed to support adaptive switch scale expansion with traffic demand increase were identified. We developed and evaluated various switch architectures for single-layer OXCs and HOXCs and the resulting levels of flexibility were discussed. We then compared switch scale, one of the most critical factors for designing switches, and clarified effective single-layer OXC and HOXC architectures in terms of switch scale and flexibility. What kinds of flexibility are needed depends on the application area, but the investigations detailed in this paper will give useful criteria to choose the most appropriate architecture to satisfy a particular request. We also evaluated switch scale with different parameters and clarified the region and the conditions in which HOXCs are more attractive than single-layer OXCs. In particular, we revealed that limiting the add/drop capability of wavelength paths at a node could greatly reduce necessary switch scale. The best way to realize the restriction in HOXC was then clarified by examining restriction at BXC level and at WXC level. We then discussed methods for realizing add/drop ports, and found that using 2×2 SWs was very effective in reducing total switch scale. These results give us important criteria regarding the introduction of the hierarchical optical path architecture and in developing truly effective HOXCs.

References

[1] D. Cooperson, "ROADM deployment plans in LH and metro networks," Proc. OFC/NFOFC, NThK3, March 2005.
[2] S. Okamoto, T. Otani, W. Imajuku, D. Shimazaki, M. Hayashi, K. Ogaki, M. Miyazawa, I. Nishioka, M. Nanba, K. Morita, S. Kano, S. Seno, K. Sagara, N. Arai, and H. Ohtsuki, "Nationwide GMPLS field trial using different types (MPLS/TDM/Lambda) of switching capable equipment from multiple vendors," Proc. OFC/NFOFC, PDP40, March 2005.
[3] L. Noirie, C. Blaizot, and E. Dotaro, "Multi-granularity optical cross-connect," Proc. Eur. Conf. Optical Communication (ECOC), pp.269–270, Oct. 2000.
[4] K. Harada, K. Shimizu, T. Kudou, and T. Ozeki, "Hierarchical optical path cross-connect systems for large scale WDM networks," Proc. OFC 1999, pp.356–358, Feb. 1999.
[5] J. Yamawaku, A. Takada, W. Imajuku, and T. Morioka, "Evaluation of amount of equipment on single-layer optical paths," J. Lightwave Technol., vol.23, no.6, pp.1971–1978, June 2005.
[6] I. Yagyu, H. Hasegawa, and K. Sato, "An efficient hierarchical optical path network design algorithm based on a traffic demand expression in a cartesian product space," Proc. Eur. Conf. Optical Communication (ECOC), pp.113–114, Sept. 2006.
[7] X. Cao, V. Anand, and C. Qiao, "Waveband switching in optical networks," IEEE Commun. Mag., vol.41, no.4, pp.105–112, April 2003.
[8] K. Sato and H. Hasegawa, "Prospects and challenges of multilayer optical networks," IEICE Trans. Commun., vol.E90-B, no.8, pp.1890–1902, Aug. 2007.
[9] A. Kolarov, T. Wang, B. Sengupta, and M. Cvijetic, "Impact of waveband switching on dimensioning multi-granular hybrid optical networks," Proc. Optical Network Design and Modeling Conference, pp.371–381, Feb. 2005.
[10] R. Izmailov, S. Ganguly, V. Kleptsyn, and A.C. Varsou, "Non-uniform waveband hierarchy in hybrid optical networks," Proc. IEEE INFOCOM, vol.2, pp.1344–1354, March 2003.
[11] C.R. Doerr, M. Cappuzzo, E. Laskowski, A. Paunescu, L. Gomez, L.W. Stulz, and J. Gates, "Dynamic wavelength equalizer in silica using the single-filtered-arm interferometer," IEEE Photonics Technol. Lett., vol.11, no.8, pp.581–583, May 1999.
[12] C.R. Doerr, R. Pafchek, and L.W. Stulz, "Integrated band demultiplexer using waveguide grating routers," IEEE Photonics Technol. Lett., vol.15, no.8, pp.1088–1090, Aug. 2003.
[13] S. Chandrasekhar, C.R. Doerr, and L.L. Buhl, "Flexible waveband optical networking without guard bands using novel 8-skip-0 banding filters," IEEE Photonics Technol. Lett., vol.17, no.3, pp.579–581, March 2005.
[14] G.J. Ockenfuss, N.A. O'Brien, and E. Williams, "Ultra-low stress

coating process: An enabling technology for extreme performance thin film interference filters," Proc. OFC 2002, PDFA8, March 2002.
[15] S. Kakehashi, H. Hasegawa, K. Sato, and O. Moriwaki, "Waveband MUX/DEMUX using concatenated arrayd-waveguide gratings," Proc. Eur. Conf. Optical Communication (ECOC), pp.233–234, Sept. 2006.
[16] S. Kakehashi, H. Hasegawa, K. Sato, O. Moriwaki, S. Kamei, Y. Jinnouchi, and M. Okuno, "Waveband MUX/DEMUX using concatenated AWGs — Formulation of waveguide connection and fabrication," Proc. OFC, March 2007.
[17] L.Y. Lin, E.L. Goldstein, J.M. Simmons, and R.W. Tkach, "Free-space micromachined optical switches with submillisecond switching time for large-scale optical crossconnects," IEEE Photonics Technol. Lett., vol.10, no.4, pp.525–527, April 1998.
[18] V. Kaman, R. Anderson, R. Helkey, O. Jerphagnon, A. Keating, B. Liu, H. Poulsen, C. Pasarla, D. Xu, S. Yuan, and X. Zheng, "Optical performance of a 288 × 288 photonic cross-connect system," Proc. PS2002, paper-PS. TuA4, pp.59–61, 2002.
[19] M. Okuno, A. Sugita, T. Matsunaga, M. Kawachi, Y. Ohmori, and K. Katoh, "8 × 8 optical matrix switch using silica-based planar lightwave circuit," IEICE Trans. Electron., vol.E76-C, no.7, pp.1215–1223, July 1993.
[20] M. Yano, F. Yamagishi, and T. Tsuda, "Optical MEMS for photonic switching-compact and stable optical crossconnect switches for simple, fast, and flexible wavelength applications in recent photonic networks," IEEE J. Sel. Top. Quantum Electron., vol.11, no.2, pp.383–394, March/April 2005.
[21] M. Okuno, T. Goh, S. Sohma, and T. Shibata, "Recent advances in optical switches using silica-based PLC technology," NTT Technical Review, vol.1, no.7, pp.20–30, Oct. 2003.
[22] S. Sohma, S. Mino, T. Watanabe, M. Ishii, T. Shibata, H. Takahashi, C.F. Lam, W. Gu, N. Hanik, and K. Oguchi, "Solid-state optical switches using planar lightwave circuit and IC-on-PLC technologies," Proc. APOC, 5625-117, pp.767–775, Nov. 2004.
[23] Y. Inoue, M. Ishii, Y. Hida, M. Yanagisawa, and Y. Enomoto, "PLC components used in FTTH access networks," NTT Technical Review, vol.3, no.7, pp.22–26, 2005.
[24] R.A. Spanke, "Architectures for guided-wave optical space switching systems," IEEE Commun. Mag., vol.25, no.5, pp.42–48, May 1987.
[25] K. Sato, Advances in Transport Network Technologies: Photonic networks, ATM, and SDH, Artech House, Norwood, 1996.
[26] P.H. Ho, T. Hussein, and J. Wu, "A scalable design of multigranularity optical cross-connects for the next-generation optical Internet," IEEE J. Sel. Areas Commun., vol.21, no.7, pp.1133–1142, Sept. 2003.
[27] R. Nagase, A. Himeno, K. Kato, and M. Okuno, "Silica-based 8 × 8 optical-matrix switch module with hybrid integrated driving circuits," Proc. Eur. Conf. Optical Communication (ECOC), Sept. 1993.
[28] W.I. Way, "ROADM technology review: Why, when, what, where, and how?," Proc. SPIE, vol.6388, pp.63880A1-A6, 2006.
[29] S. Okamoto, A. Watanabe, and K. Sato, "A new optical path cross-connect system architecture utilizing delivery and coupling matrix switch," IEICE Trans. Commun., vol.E77-B, no.10, pp.1272–1274, Oct. 1994.
[30] K. Sato, "Prospects and challenges of photonic IP networks," Proc. Asia-Pacific Optical Communications Conference (APOC) 2004, pp.382–390, Nov. 2004.
[31] G. Cambron, "The multimedia explosion: Transforming the physical layer," Proc. OFC 2006, March 2006.
[32] L. Noirie, M. Vigoureux, and E. Dotaro, "Impact of intermediate traffic grouping on the dimensioning of multi-granularity optical networks," Proc. Optical Fiber Communication (OFC), pp.TuG3/1–3, March 2001.
[33] V. Kaman, X. Zheng, O. Jerphagnon, C. Pusarla, R.J. Helkey, and J.E. Bowers, "A cyclic MUX-DMUX photonic cross-connect architecture for transparent waveband optical networks," IEEE Photonics Technol. Lett., vol.16, no.2, pp.638–640, Feb. 2004.

Appendix

Table A·1 Formulation for switch scale.

Figure	Switch scale
Fig. 3	$2M^2N^2(1+x)^2$
Fig. 4	$8MN^2+4M^2N^2x$
Fig. 5	$2MN^2(1+x)^2$
Fig. 6	$MN^2(1+x)^2$
Fig. 9	$8KN^2+4K^2N^2y+2M^2N^2y^2(1+z)^2$
Fig. 10	$2KN^2(1+y)^2+2MN^2y^2(1+z)^2$
Fig. 11	$KN^2(1+y)+KN^2y+2M^2N^2y^2(1+z)^2$

K: number of wavebands per fiber
M: number of wavelengths per fiber
N: number of fiber
x: ratio of wavelength paths to be added/dropped for connections to electrical systems to that coming/outgoing to/from the node
y: ratio of WBs that are added from WXC to BXC, to WBs that are launched from the node
z: ratio of wavelength paths that are added from electrical systems to WXC, to the wavelength paths that are added from WXC to BXC

Shoji Kakehashi was born in 1983. He graduated from the Nagoya University, department of ECCS in 2006 and presently he is a graduate student of the department. His major interests include photonic network node architecture, wavelength routing devices, and the optical performances. He is a member of IEEE.

Hiroshi Hasegawa received the B.E., M.E., and D.E. degrees all in Electrical and Electronic Engineering from Tokyo Institute of Technology, Tokyo, Japan, in 1995, 1997, and 2000, respectively. From 2000 to 2005, he was an assistant professor of Dept. of Communications and Integrated Systems, Tokyo Institute of Technology. Currently he is an associate professor of Nagoya University. His current research interests include Photonic Networks, Image Processing (especially Super-resolution), Multidimensional Digital Signal Processing and Time-Frequency Analysis. He received the Young Researcher Awards from SITA (Society of Information Theory and its Applications) and IEICE (Institute of Electronics, Information and Communication Engineers) in 2003 and 2005, respectively. Dr. Hasegawa is a member of SITA and IEEE.

Ken-ichi Sato is currently a professor at the graduate school of Engineering, Nagoya University, and he is an NTT R&D Fellow. Before joining the university in April 2004, he was an executive manager of the Photonic Transport Network Laboratory at NTT. His R&D activities covers future transport network architectures, network design, OA&M (operation administration and maintenance) systems, photonic network systems including optical cross-connect/ADM and photonic IP routers, and optical transmission technologies. He has authored/co-authored more than 200 research publications in international journals and conferences. He holds 35 granted patents and more than 100 pending patents. He received his B.S., M.S., and Ph.D. degrees in electronics engineering from the University of Tokyo, Tokyo, Japan, in 1976, 1978, and 1986, respectively. He received the Young Engineer Award in 1984, the Excellent Paper Award in 1991, and the Achievement Award in 2000 from the Institute of Electronics, Information and Communication Engineers (IEICE) of JAPAN. He was also the recipient of the distinguished achievement Award of the Ministry of Education, Science and Culture in 2002. His contributions to ATM (Asynchronous Transfer Mode) and optical network technology development extend to co-editing three IEEE JSAC special issues and the IEEE JLT special issue once, organizing several Workshops and Conference technical sessions, serving on numerous committees of international conferences including OFC and ECOC, authoring a book, Advances in Transport Network Technologies (Artech House, 1996), and co-authoring thirteen other books. He is a Fellow of the IEEE.